AIAA SciTech Forum
5-9 January 2015, Kissimmee, Florida
2nd AIAA Spacecraft Structures Conference

Spin-Stabilized Membrane Antenna Structures

M. Delapierre* and S. Pellegrino†
California Institute of Technology, Pasadena, CA 91125

This paper explores the possibility of using spin-stabilized membrane structures for large phased array microwave antennas (typically L-Band or S-Band from 1 GHz to 4 GHz). The biggest challenge is to be able to sufficiently stabilize the system in order to limit its sensitivity to space disturbances (maneuvering, reaction wheels, and other imposed forces) and manufacturing imperfections. First, a flatness requirement for microwave antennas is derived. Then a frequency analysis of isotropic flat structures spinning at different angular velocities and with different bending stiffnesses is carried out. These analyses, together with finite element simulations, are used to derive scaling laws to study the behavior of large spinning structures. A test case, based on a spinning structure perturbed at the hub, is considered. An analytical solution of the free vibration of this test case is compared to the results of finite-element method simulations with Abaqus/Standard. Finally a test setup to study the dynamics of scaled spinning membranes in the laboratory is presented. Gravity effects in such an experiment are expected to be small.

Nomenclature

a	Inner Radius	γ	Non dimensional frequency
b	Outer radius	η	Gravity parameter
D	Bending stiffness	κ	Stiffness parameter
E	Young's modulus	λ	Wavelength
f	Frequency	ν	Poisson's ratio
g	Gravity	ρ	Density (kg.m^{-3})
h	Thickness	σ_r	Radial component of in-plane stress due to centrifugal force
n	Number of nodal circles	σ_θ	Circumferential component of in-plane stress due to centrifugal force
p_0	Perturbation	σ_r^g	Radial component of in-plane stress due to gravity
s	Number of nodal diameters	σ_θ^g	Circumferential component of in-plane stress due to gravity
w	Out of plane displacement	ω	Angular velocity
α	Radius ratio		

I. Introduction and Background

Membrane-like space structures are used for many applications, such as sunshields, solar sails, patch antennas and solar arrays. In recent years there has been significant activity and many advance in solar sails. In 2005 NASA tested two square sails under thermal vacuum conditions, the ATK 20 m concept (figure 1) and the L'Garde 20 m concept (figure 2). Both of these prototypes were deployed and stabilized by means

*Graduate student, Graduate Aerospace Laboratories, 1200 E. California Blvd, MC 105-50. delapmel@caltech.edu
†Joyce and Kent Kresa Professor of Aeronautics and Professor of Civil Engineering, Graduate Aerospace Laboratories, 1200 E. California Blvd, MC 301-46. AIAA Fellow. sergiop@caltech.edu

of deployable booms. Ultra-light graphite coilable booms were used for the ATK system and inflatable lightweight booms with sub-Tg rigidization for the L'Garde system. In 2010 JAXA deployed in space a 20 m diagonal spinning solar sail for a deep space mission. Instead of using booms to deploy the IKAROS sail, the deployment was actuated by the centrifugal forces generated by four tip masses attached to the vertexes of the square sail. After deployment the system continues to spin at 1-2 rpm.

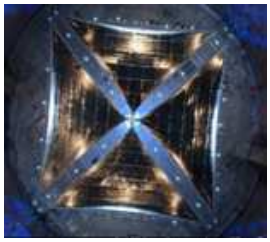

Figure 1: ATK 20 m

Figure 2: L'Garde 20 m

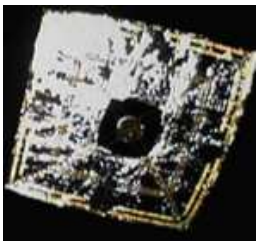

Figure 3: IKAROS 14 m

The aim of the paper is to study the dynamics of spinning membrane-like structures for applications such as space-based microwave phased array antennas. As a specific example, a continuous isotropic structure clamped to a central hub is considered. Following the derivation of a coarse stability requirement for phased array antennas, an analytical study of the linearized dynamics of a perfect spinning membrane subject to a specific type of disturbance is presented. The study considers the asymptotic behaviors of thick membranes, whose behavior is dominated by bending stiffness, and thin membranes, whose behavior is dominated by the inertia forces generated by spinning membranes. Numerical simulations that include geometrically non-linear effects are also carried out with the Abaqus/Standard finite element software. The influence of numerical damping on the precision of several implicit integration schemes is evaluated and the influence of large amplitudes on the natural frequencies of vibration of the membrane is investigated. Finally, a design of a laboratory scale experiment to study the dynamics of spinning membrane with only minimal gravity-induced disturbances is carried out.

II. Stability Requirement for Microwave Phased Array Antennas

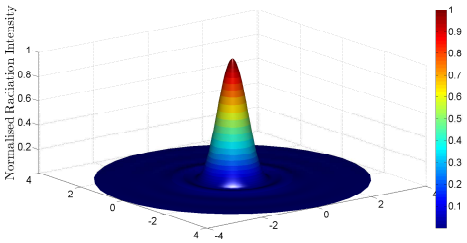

Figure 4: Radiation pattern of flat structure.

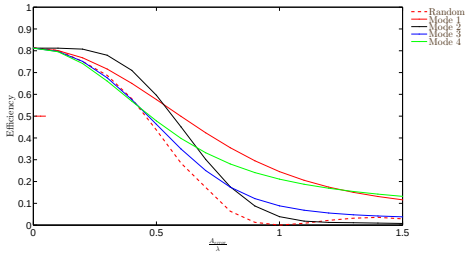

Figure 5: Efficiency sensitivity to shape deformation on the first 4 vibration modes

The stability requirement for an antenna depends on its size, purpose and wavelength of operation. For example, consider a phased array of square patch antennas on a grid of $\frac{\lambda}{2}$ with $\lambda \simeq 30$ cm (1 GHz microwaves), attached to a 60 m diameter spinning membrane structure. The antennas are synchronized to emit coherently, in order to transmit power in a narrow beam. If the calibration of the antennas is carried out assuming that the membrane structure is perfectly planar, a subsequent distortion of the structure distorts the radiation pattern and causes some power to be lost.

The efficiency of the array antenna is defined as the capability of transferring power in a chosen direction, which corresponds to the direction of the main beam if the antenna is perfectly planar. Figure 4 shows the normalized radiation pattern (normalized radiation intensity in every direction) of a calibrated flat structure for λ=1 m (faster simulations). Figure 5 shows the power transmission efficiency of the 60 m antenna array respectively deformed on each of the first vibration modes of a spinning membrane as a function of the

deformation amplitude along with random deformation of various amplitudes. The x-axis is the amplitude of the mode (maximum out-of-plane deformation) divided by the wavelength. In particular, for λ=30 cm the figure shows that a shape error of 18 cm over a 60 m structure decreases the power efficiency by a factor of two for at least one mode. This observation drives the requirement that the structure must be stable to a few centimeters for this application.

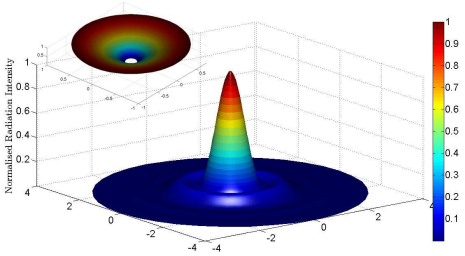

Figure 6: Radiation pattern for structure deformed according to Mode 1, with amplitude $\frac{\lambda}{2}$.

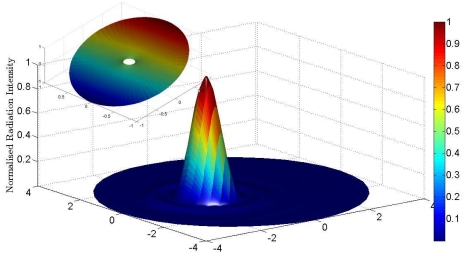

Figure 7: Radiation pattern for structure deformed according to Mode 2, with amplitude $\frac{\lambda}{2}$.

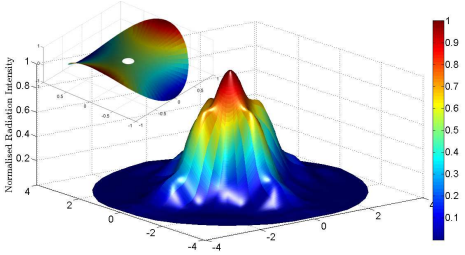

Figure 8: Radiation pattern for structure deformed according to Mode 3, with amplitude $\frac{\lambda}{2}$.

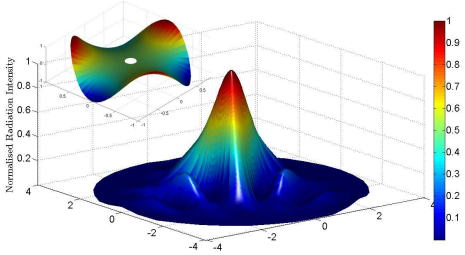

Figure 9: Radiation pattern for structure deformed according to Mode 4, with amplitude $\frac{\lambda}{2}$

This example highlights the importance of maintaining geometrical stability in large spinning membrane-like structures.

III. Dynamics of Spinning Membrane Structures

There are two effects that stabilize the spinning membrane structure shown in figure 10, centrifugal force and bending stiffness. We can solve the linear dynamic equation for both of these asymptotic behaviors using a series expansion in one case and Bessel functions in the other. The actual structure behavior can be analyzed using finite element methods.

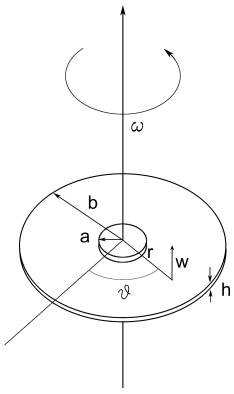

Figure 10: Definition of geometry and variables.

A. Static Plate Behavior

The linear dynamics of a thin annulus is a classical problem that has been solved analytically. Leissa[6] solves a wide range of problems, in particular the annulus clamped at the hub and free at the edge using Bessel functions. The classical differential equation of motion for the transverse displacement w of a thin plate is given by:

$$D\nabla^4 w + \rho h \frac{\delta^2 w}{\delta t^2} = 0 \tag{1}$$

where D is the bending stiffness:

$$D = \frac{Eh^3}{12(1-\nu^2)} \tag{2}$$

The boundary conditions are:

$$\text{clamped at} \quad r = a: \quad \begin{cases} W(a,\theta) = 0 \\ \frac{\delta}{\delta r} W(a,\theta) = 0 \end{cases}$$

$$\text{free at} \quad r = b: \quad \begin{cases} M_r(b,\theta) = 0 \\ V_r(b,\theta) = 0 \end{cases}$$

where M_r is the bending moment and V_r the Kelvin-Kirchhoff edge reaction.

For free vibration we expand w in terms of Fourier components in θ and thus the solution takes the following form:

$$w = \cos(2\pi f t) W(r,\theta) \tag{3}$$

$$= \cos(2\pi f t)\left(\sum_{s=0}^{\infty} W_s(r)\cos(s\theta) + \sum_{s=0}^{\infty} W_s^*(r)\sin(s\theta)\right) \tag{4}$$

Where s is the number of nodal diameters. Substituting equation 3 into equation 1 we find an identical system of equations for W_s and W_s^*, whose solutions are expressed in term of the Bessel's functions:

$$W_{s1} = A_s J_s(kr) + B_s Y_s(kr) \tag{5}$$

$$W_{s2} = C_s I_s(kr) + D_s K_s(kr) \tag{6}$$

with

$$k^4 = \frac{\rho h (2\pi f)^2}{D} \tag{7}$$

A_s, B_s, C_s, D_s are obtained by considering the boundary conditions.

For a non-trivial solution to exist the determinant of the 4×4 matrix expressing the boundary conditions must be zero. From this condition we can solve for the non-dimensional frequencies $\gamma = kb$ defined as

$$\gamma^2 = b^2 2\pi f \sqrt{\frac{\rho h}{D}} \tag{8}$$

We solve the problem with Matlab for $s = 0, \ldots 4$ and $n = 0, \ldots 3$ (n is the number of nodal circles). Figure 11 shows a plot of γ for different values of $\alpha = a/b$ and for $\nu = 0.34$.

B. Spinning Membrane Behavior

If the structure is thin then its bending stiffness can be neglected and the dynamics are dominated by the pre-stress due to the centrifugal force. The linear equation of the out of plane deformation w is then governed by the second-order equation

$$\frac{h}{r}\frac{\delta}{\delta r}(r\sigma_r \frac{\delta w}{\delta r}) + \frac{h}{r^2}\frac{\delta}{\delta \theta}(\sigma_\theta \frac{\delta w}{\delta \theta}) - \rho h \frac{\delta^2 w}{\delta t^2} = 0 \tag{9}$$

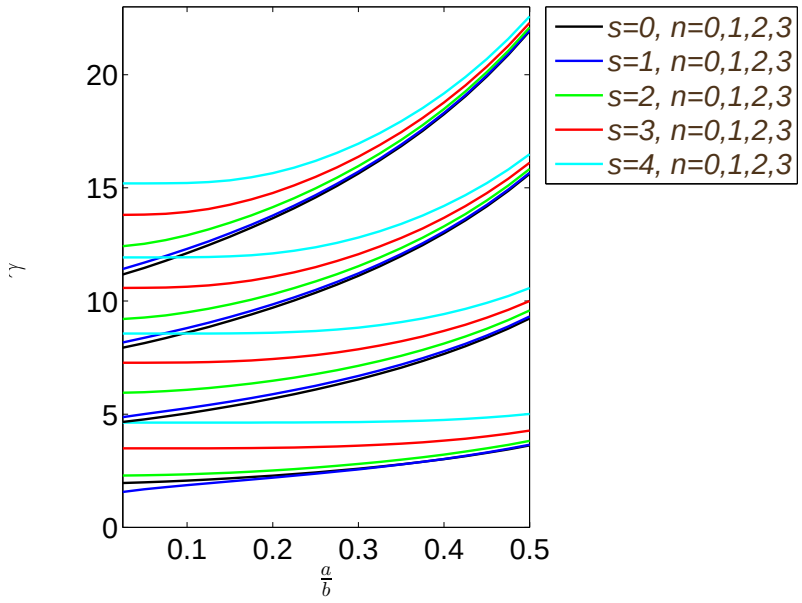

Figure 11: Non-dimensional frequencies of circular plate with ν=0.34.

The stress components σ_r and σ_θ have the expressions

$$\sigma_r(r) = \rho\omega^2 b^2 (A[\nu](\frac{r}{b})^2 + B[\nu,\alpha] + C[\nu,\alpha](\frac{b}{r})^2) \tag{10}$$

$$= \rho\omega^2 b^2 P_{\nu,\alpha}[\bar{r}] \tag{11}$$

$$\sigma_\theta(r) = \rho\omega^2 b^2 (D[\nu,\alpha](\frac{r}{b})^2 + E[\nu,\alpha] + F[\nu,\alpha](\frac{b}{r})^2) \tag{12}$$

$$= \rho\omega^2 b^2 Q_{\nu,\alpha}[\bar{r}] \tag{13}$$

with $\bar{r} = r/b$.

The boundary conditions are

$$\begin{cases} W(a,\theta) = 0 \\ W(b,\theta) = \text{finite} \end{cases}$$

We once again expand the solution in terms of Fourier components in θ. The resulting second-order equation and boundary conditions constitute a Sturm-Liouville problem with a regular singular point. We refer to the technical note by Eversman[4] to solve the problem by series expansion. We first do a change of variable to express W between 0 and 1 and put the singularity at 0:

$$\zeta = \frac{1-\bar{r}^2}{1-\alpha^2} \tag{14}$$

with boundary conditions:

$$\begin{cases} W(0) = \text{finite} \\ W(1) = 0 \end{cases}$$

This problem can be solved with the following series expansion:

$$W = \sum_{n=0}^{\infty} C_n \zeta^n \tag{15}$$

Hence we evaluate with Matlab the non-dimensional frequencies for $s = 0, \ldots 3$ and $n = 0, \ldots 2$ according to $\alpha \in [0, 0.5]$ and ν=0.34. The results are plotted in figure 12. It should be noted that there may exist lower frequencies, corresponding to higher values of s, which have not been calculated.

We also plot the radial variation of the first five axisymmetric modes in figure 13.

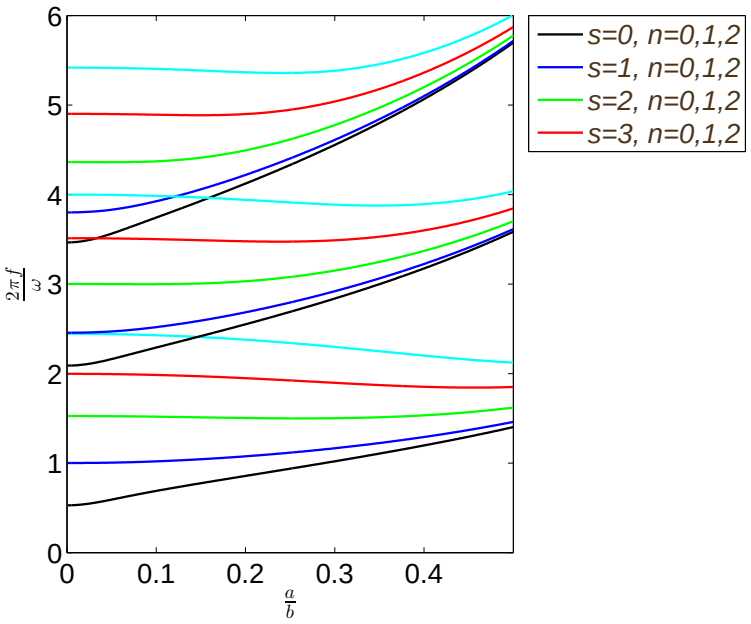

Figure 12: Non-dimensional frequencies of circular membrane spinning at ω with ν=0.34.

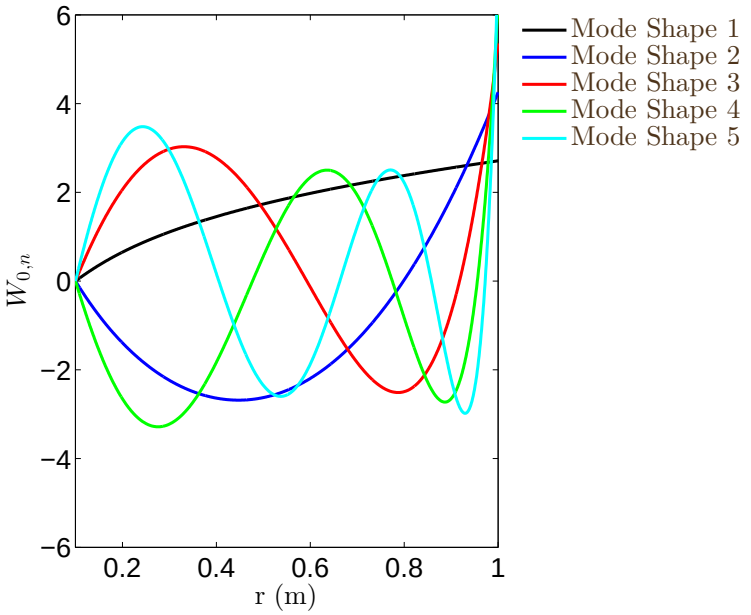

Figure 13: Radial variation of first five axisymmetric modes for a spinning membrane with ν=0.34.

C. Spinning Plate Behavior

The differential equation of motion for the transverse displacement w of a spinning plate is given by:

$$D\nabla^4 w - \frac{h}{r}\frac{\delta}{\delta r}(r\sigma_r\frac{\delta w}{\delta r}) - \frac{h}{r^2}\frac{\delta}{\delta\theta}(\sigma_\theta\frac{\delta w}{\delta\theta}) + \rho h\frac{\delta^2 w}{\delta t^2} = 0 \tag{16}$$

which gives for free vibrations:

$$D\nabla^4 W - \frac{h}{r}\frac{\delta}{\delta r}(r\sigma_r\frac{\delta W}{\delta r}) - \frac{h}{r^2}\frac{\delta}{\delta\theta}(\sigma_\theta\frac{\delta W}{\delta\theta}) + \rho h(2\pi f)^2 W = 0 \tag{17}$$

The associated boundary conditions are:

$$\begin{cases} W(a,\theta)=0 \\ \frac{\delta}{\delta r}W(a,\theta)=0 \\ M_r(b,\theta)=0 \\ V_r(b,\theta)=0 \end{cases}$$

We can non-dimensionalize this equation for each mode by using $\bar{r}=\frac{r}{b}$ and $\bar{t}=\omega t$, and obtain the following equation for the eigenmodes of the system.

$$\kappa\nabla^4 W-\frac{1}{\bar{r}}\frac{\delta}{\delta\bar{r}}(\bar{r}P_{\nu,\alpha}(\bar{r})\frac{\delta W}{\delta\bar{r}})-\frac{1}{\bar{r}^2}\frac{\delta}{\delta\theta}(Q_{\nu,\alpha}(\bar{r})\frac{\delta W}{\delta\theta})+W=0 \tag{18}$$

With the associated non-dimensional boundary conditions:

$$\begin{cases} W(\alpha,\theta)=0 \\ \frac{\delta}{\delta\bar{r}}W(\alpha,\theta)=0 \\ M_r(1,\theta)=0 \\ V_r(1,\theta)=0 \end{cases}$$

and the stiffness parameter

$$\kappa=\frac{Eh^2}{\rho b^4\omega^2} \tag{19}$$

Thus, the eigenmodes of the spinning plate depend only on α, ν and κ.

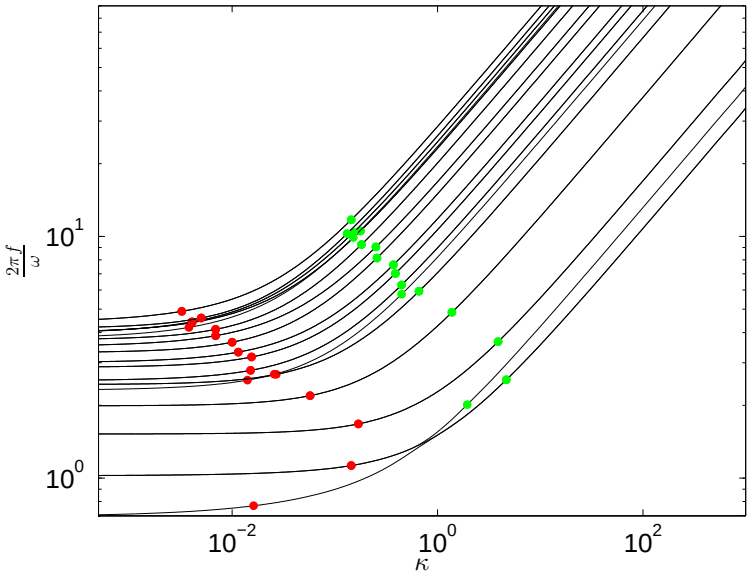

Figure 14: Influence of stiffness parameter on the first non-dimensional frequencies, for the case α=0.1 and ν=0.34.

The first non-dimensional frequencies of a spinning plate are plotted in figure 14 according to κ (with α=0.1 and ν=0.34). In particular, when κ is very small we find the linear dynamics of a spinning membrane and:

$$\frac{2\pi f}{\omega}=C_i \tag{20}$$

When κ is large we are in the static plate regime and:

$$\frac{2\pi f}{\omega}=D_i\sqrt{\kappa} \tag{21}$$

where C_i and D_i depend on the mode, α and ν. C_i is plotted in figure 12 and $D_i=\frac{\gamma^2}{12(1-\nu^2)}$ in figure 11.

The red dots in figure 14 represent, for each mode, the value of κ at which the frequency is within 10% of the spinning membrane case and the green dots mark the values of κ at which the frequency is within 10% of the static plate solution.

More generally two systems with the same κ have the same linearized dynamics. This is the criterion we use to scale our experiments. In particular, the dynamics of a 60 m diameter, 3 mm thick Kapton membrane with a 3 m diameter hub, spinning at 1 rpm has $\kappa = 2\times10^{-4}$. Any system with $\kappa = 2\times10^{-4}$ would have the same linearized dynamics and, at least for the first 16 modes —plotted in figure 14— the dynamic regime is that of a spinning membrane.

IV. Description and Analytical Solution of a Test Case

Consider a circular membrane spinning at $\omega = 150$ rad s^{-1}. The membrane is initially flat and clamped to a central the hub, figure 10. We apply a vertical step displacement, p_0, at the hub and let the structure vibrate freely. Only the axisymmetrical modes are excited. We solve this problem analytically by mode superposition to evaluate the weight of each axisymmetric mode on the vibration.

The spatial boundary condition being non-homogeneous, we apply the modal expansion that we found in Section III-B. The imposed boundary conditions are:

$$\begin{cases} W(a) = P(t) \\ W(b) = \text{finite} \end{cases}$$

with

$$\begin{cases} P(t) = 0 & t < 0 \\ P(t) = p_0 & t \geq 0 \end{cases}$$

and the initial conditions are:

$$\begin{cases} W(r,\theta,0) = 0 \\ \dot{W}(r,\theta,0) = 0 \end{cases}$$

Hence, the out-of-plane displacement is independent of θ and can be expressed as:

$$W(r,t) = W_{qs}(r,t) + \sum_{n=0}^{\infty} \eta_n(t) W_{0,n}(r) \tag{22}$$

where $W_{qs}(r,t) = p_0$ is the quasi-static solution and $W_{0,n}(r)$ are the normalized eigenmodes for s=0.

As the initial conditions are zero and there is no body force we can express equation 22 as:

$$W(r,t) = p_0 + \sum_{n=0}^{\infty} W_{0,n}(r) cos(\omega_{0,n} t) \int_V \rho W_{0,n}(r)(-p_0) dV \tag{23}$$

$$= p_0 - p_0 \rho h 2\pi \sum_{n=0}^{\infty} W_{0,n}(r) cos(\omega_{0,n} t) \int_a^b W_{0,n}(r) r dr \tag{24}$$

To find the weight of each mode we first normalize the mode shapes from Section III-B with:

$$\int_a^b \rho 2\pi h W_{0,n}^2(r) r dr = 1 \tag{25}$$

The weight of each mode at $r = b$ is

$$B_n = A_n W_{0,n}(b) \tag{26}$$

with

$$A_n = \rho 2\pi h \int_a^b W_{0,n}(r) r dr \tag{27}$$

The results are plotted in figure 15 for the particular case $\omega = 150$ rad s^{-1}. This results are our baseline solution to validate the finite element method simulations presented in the next section.

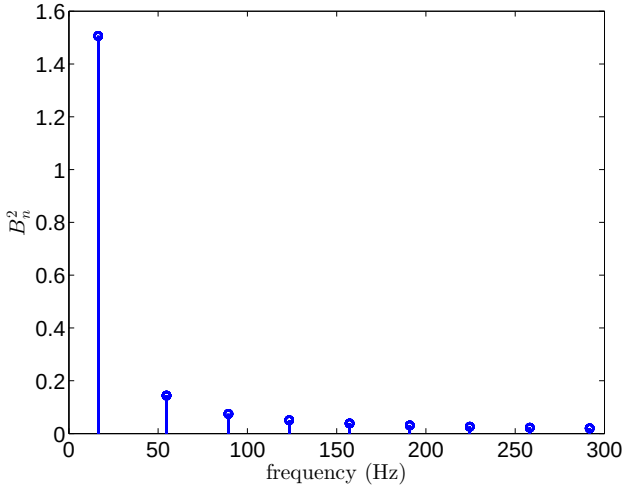

Figure 15: Weight of first modes on the response at r=b

V. Numerical Simulations

We have set up the study case described in Section IV in the finite element software Abaqus/Standard. We use this example to study the influence of numerical damping on the precision of the results and the time of the simulation. Then we study the non-linear effects of the response of the system for the first axisymmetric modes.

A. Simulation Description

We consider a 40 cm diameter, 50 μm thick disk made of Kapton with a 4 cm diameter hub at the center. Its properties and dimensions are provided in Table 1. They correspond to the ones of the experimental setup as explained in the next part. The hub is defined by a set of constrained nodes using the RIGID BODY option. We use a regular mesh with 10 elements radially and 40 circumferentially. The elements used are shell elements S4R (a 4-node thick shell element, with reduced integration, hourglass control, finite membrane strain formulation).

E	2.5 GPa
ν	0.34
ρ	1420 kg m^{-3}
h	50 μm
b	20 cm
a	2 cm

Table 1: Geometry and properties of test case.

We simulate the non-linear dynamics with the NLGEOM option. We impose the initial conditions using a PREDEFINED FIELD and then run a dynamic implicit step. The predefined field corresponds to a perfectly flat structure spinning at 150 rad s^{-1}.

We use three integration schemes to compute the dynamic response: Backward Euler, HHT (Hilbert, Hughes and Taylor) with α=0.33, HHT with α=0.05, HHT with α=0. After 0.1 s we perturb the hub vertically, moving it by p_0=1 μm over 0.0004 s. We then let the simulation run for 0.3 s with a maximal increment step of 0.0004 s (to be able to perform a precise fft on the obtained signal).

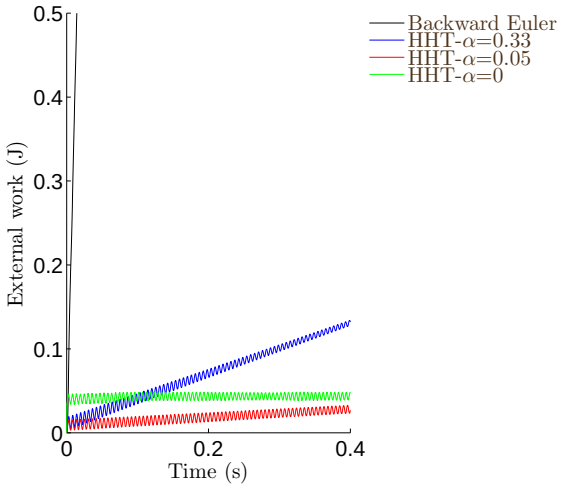

Figure 16: External work.

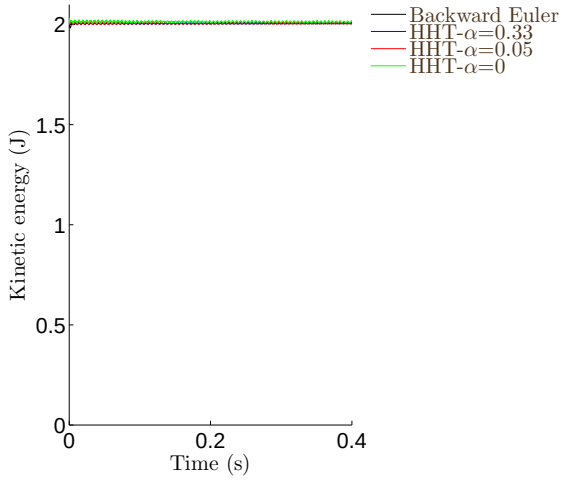

Figure 17: Kinetic energy.

B. Numerical Damping

We compare the time needed to execute the simulation for a perturbation p_0=1 μm, provided in table 2, and the precision of the results of the various integration schemes. The Backward Euler and the HHT integrations for $\alpha = 0.33,\ 0.05$ take about 5 min while HHT with $\alpha = 0$ takes 30 min.

Scheme	CPU Time (s)
Backward Euler	376
HHT-α=0.33	303
HHT-α=0.05	302
HHT-α=0	2461

Table 2: Simulation times.

Figures 16 and 17 show plots of the total external work and kinetic energy of the whole structure. The external work should remain constant, but only the simulations with the lowest damping captures this behavior almost correctly (green plot, which however was obtained from a simulation with a heavier hub).

Figure 18 shows a plot of the out of plane displacement at the extremity of the disk. As only the axisymmetric modes are excited we have plotted the displacement at a material point on the membrane, as in this particular case there is no difference if we follow a point on the spinning disk.

Figure 19 presents the Fourier transform of the signal, computed with the fft function in Matlab. Note that the solution based on the Backward Euler scheme identifies only the two dominant modes; the remaining are heavily damped. The HHT scheme with $\alpha = 0.05$ identifies at least the first 9 modes. The analytical and simulated results are compared in table 3. All the results are within an error smaller than 9%. The HHT scheme with $\alpha = 0$ identifies many more modes, possibly because non-symmetric modes have been excited due to the difficulty of setting up perfect initial conditions, or because of convergence/noise issues during the integration.

Finally, figure 20 compares the relative weight of the first modes obtained with HHT-α=0.05 with the analytical ones. Notice that the higher frequencies components identified by the analytical solution are over-damped in the numerical solution. Despite this drawback, the HHT scheme with α=0.05 was chosen for the next set of simulations as it is fast, robust to initial imperfections and gives good precision for the first two frequencies.

Mode no.	Analytic (Hz)	HHT-α=0.05 (Hz)
1	16.46	16.6
2	54.69	53.03
3	89.36	83.84
4	123.42	112.4
5	157.258	144.6
6	190.96	178.4
7	224.59	218.2
8	258.18	251.6
9	291.74	294.8

Table 3: Comparison of frequencies below 300 Hz.

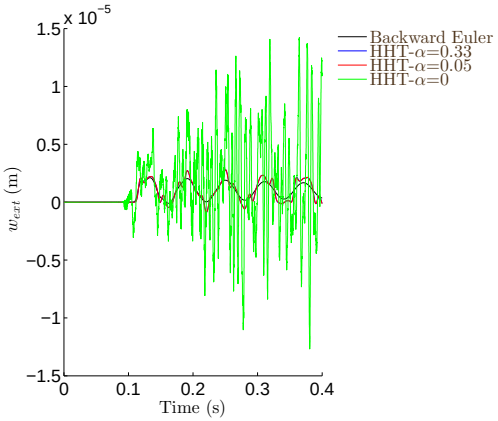

Figure 18: Out of plane displacement at the extremity.

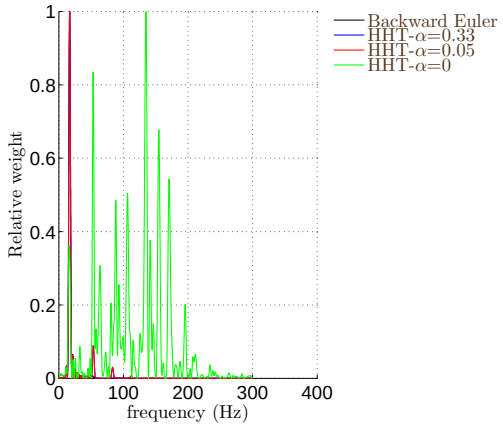

Figure 19: Dominant frequencies of the response.

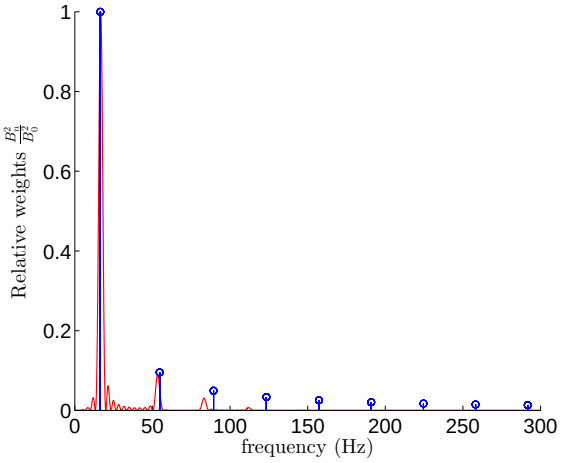

Figure 20: Frequency content of responses obtained from analytical solution (blue) and simulation with HHT with $\alpha = 0.05$ (red).

C. Non-Linear Effects

When the amplitude of the perturbation is increased the deformation of the membrane grows bigger and hence the small amplitude hypothesis doesn't hold anymore as the behavior becomes non-linear. To study this effect, we run our simulation for p_0 between 1 μm and 2 mm. The results are shown in figure 21. In figure 22 we plot the weight of the modes in each signal normalized by the weight of the modes obtained in the linear case. In these two sets of plots, notice a shift in the frequencies and relative amplitudes. Using these results, we can also estimate that the range of disturbances for which the response remains linear is up to 100 μm (twice the thickness of the membrane).

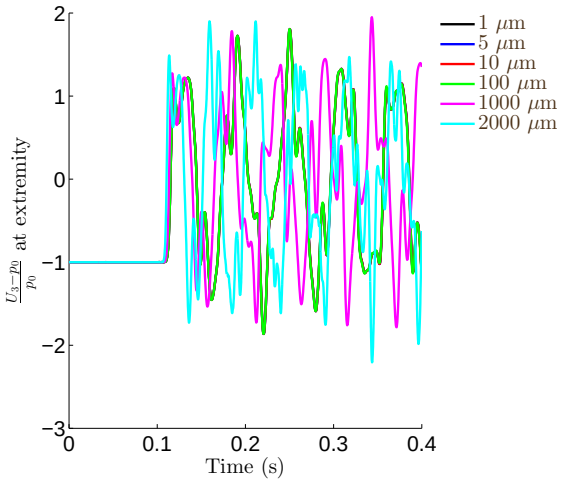

Figure 21: Free vibration for different amplitudes of perturbation

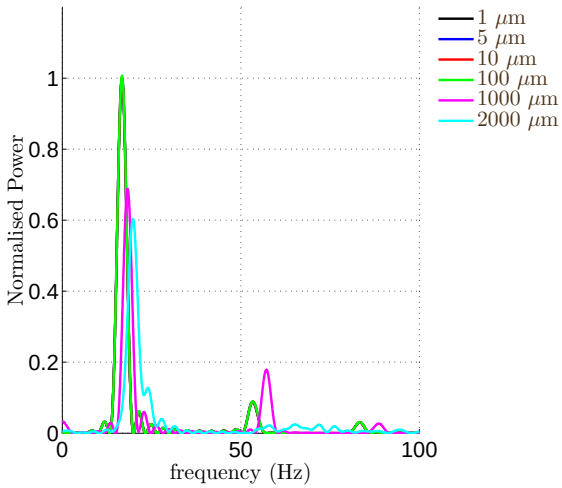

Figure 22: fft of the free vibration for different amplitudes of perturbation

VI. Experiments

We would like to recreate in the laboratory the dynamics of a 60 m spinning membrane with low gravity effects. It was explained in Section III that this problem can be scaled to a smaller geometry. To maintain the same linearized dynamics we need to keep $\kappa = 2 \times 10^{-4}$ while rescaling. In this section we study the influence of gravity on our system and the range of test parameters for which gravity effects can be neglected. Another challenge is the design of an experiment that creates the appropriate initial conditions for a spinning test.

A. Gravity Effect

We can either spin the structure horizontally (gravity out of plane) or vertically (gravity in plane). We describe here the influence of gravity in these two cases and derive a criterion for neglecting gravity.

1. *In-plane Gravity*

When we spin the membrane in a vertical plane, gravity acts in-plane and changes the equilibrium stress within the structure. The dynamical equation is the same as equation 16 with a modified equilibrium stress. If the structure stays vertical (centrifugal effects larger than gravitational effects) the stress can be expressed by superposition as:

$$\sigma(r,\theta) = \sigma(r) + \sigma^g(r,\theta) \tag{28}$$

where

$$\sigma^g(r,\theta) = \rho g b f_g[\frac{r}{b}, \theta, \nu] \tag{29}$$

Hence, the linearized dynamics can be expressed in non-dimensional form as:

$$\kappa\nabla^4 W - \frac{1}{\bar{r}}\frac{\delta}{\delta\bar{r}}(\bar{r}P_{\nu,\alpha}(\bar{r})\frac{\delta W}{\delta\bar{r}}) - \frac{1}{\bar{r}^2}\frac{\delta}{\delta\theta}(Q_{\nu,\alpha}(\bar{r})\frac{\delta W}{\delta\theta}) - \eta(\frac{1}{\bar{r}}\frac{\delta}{\delta\bar{r}}(\bar{r}f_{g,r}\frac{\delta W}{\delta\bar{r}}) + \frac{1}{\bar{r}^2}\frac{\delta}{\delta\theta}(f_{g,\theta}\frac{\delta W}{\delta\theta})) + W = 0 \quad (30)$$

with:

$$\eta = \frac{g}{b\omega^2} \quad (31)$$

In this case, the linearized dynamics are controlled by the two parameters κ and η.

We evaluate with Abaqus the error introduced by in-plane gravity on the response of the lowest modes. The largest influence is on the fourth frequency (over the first five) and is shown in figure 24. In particular, for $\kappa = 2 \times 10^{-4}$ if η is smaller than 0.1, gravity introduces an error smaller than 10 %.

We obtain the two following relations to design our experiment:

$$\kappa = 2 \times 10^{-4} \quad (32)$$

$$\eta < 0.1 \quad (33)$$

Hence, if we choose a Kapton membrane with diameter of 40 cm, we find that to satisfy these conditions we need to spin a 50 μm thick structure at 23 rad s^{-1}.

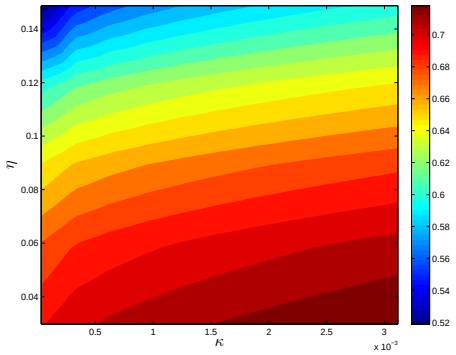

Figure 23: Variation of fourth natural frequency with κ and η, for α=0.1 and ν=0.34

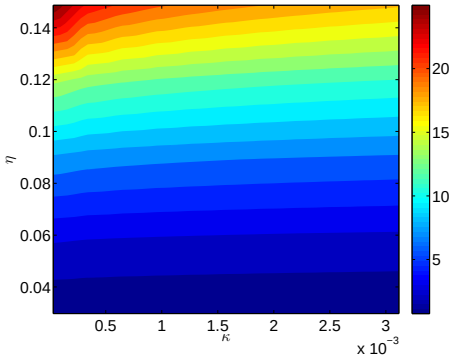

Figure 24: Variation of error on fourth natural frequency with κ and η, for α=0.1 and ν=0.34

2. *Out-of-plane Gravity*

When we spin the membrane in a horizontal plane, gravity acts out of plane and the stress distribution is changed. Instead of carrying out a general study, we have considered the influence of gravity on a 40 cm diameter Kapton membrane with a 4 cm hub. The variables in our design are the thickness and angular velocity. We would like the angular velocity to be as small as possible which would simplify the image acquisition and a thickness that corresponds to existing Kapton film (as thick as possible to limit the sensitivity to imperfection and kinks).

We have evaluated with Abaqus/Standard the error due to gravity on the first 5 modes for $\omega \in$ [80 300] rad s^{-1} and $h \in$ [10 μm 1 mm]. The relative error for the first frequency is presented in figure 25. The green line corresponds to the membrane approximation limit defined by the red dots in figure 14 and the red line corresponds to the value of κ we are interested in. On figure 26 we represent the 10 % error limit for the first 5 modes.

In particular, a 40 cm diameter membrane with a 4 cm hub, 50 μm thick spinning at 150 rad s^{-1} would recreate the linearized dynamics of a 60 m system with minimal gravity effects.

In principle it seems easier to spin the membrane vertically. Nevertheless it is easier to keep the structure flat using a support plate if we spin it horizontally, as described in next section. For now, we consider for our experiments a 40 cm diameter, 50 μm thick Kapton membrane with a 4 cm hub, spinning at 150 rad s^{-1} horizontally.

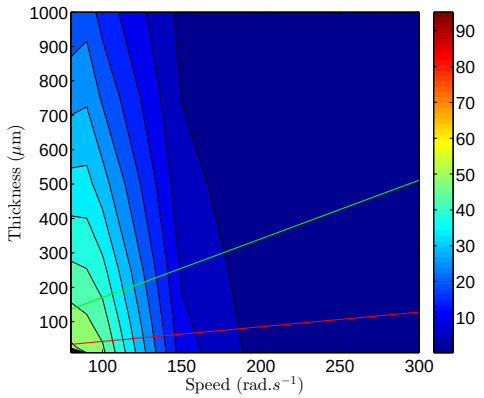

Figure 25: Error due to out of plane gravity on mode 1.

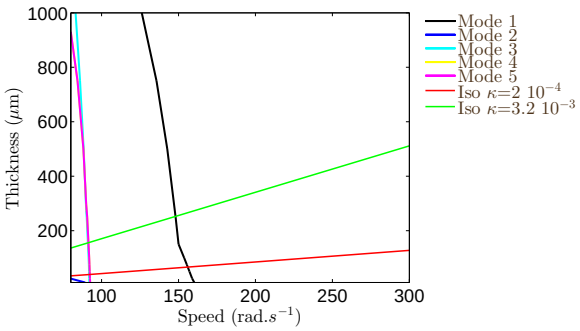

Figure 26: 10% error limit on first 5 modes.

B. Setup Description

The main challenges of setting up a lab experiment are to decouple the source of rotation (electric motor) from the vertical motion (shaker) and to set up a flat or nearly flat membrane spinning at 150 rad s^{-1}. We decouple rotation and linear motion with a system of gears and ball splines (a related study can be found in reference[12]).

To keep the membrane flat during spin up we support it on an aluminum plate. This support is removed once the structure has sufficiently high inertia-induced stresses to be able to sustain itself and gravity effects are negligible on the linear dynamics (which happens when the membrane spins at 150 rad s^{-1}).

A compact test setup, shown in figure 27, has been designed. It can be automatized to fit and operate in a vacuum chamber. The blue components move only vertically; red components rotate only; and the purple parts (mainly the shaft and the hub) and the orange part (membrane) both rotate and move vertically. The height of the support plate is controlled by three vertical rods attached to vertical actuators (only one is represented in the figures); each rods is terminated with a ball bearing. We lower the support plate after spinning up the membrane, the rods are lowered by 1 cm. Note that this test rig allows unobscured views of the top side of the membrane, which can be imaged with a high speed digital image correlation system to identify the vibration modes.

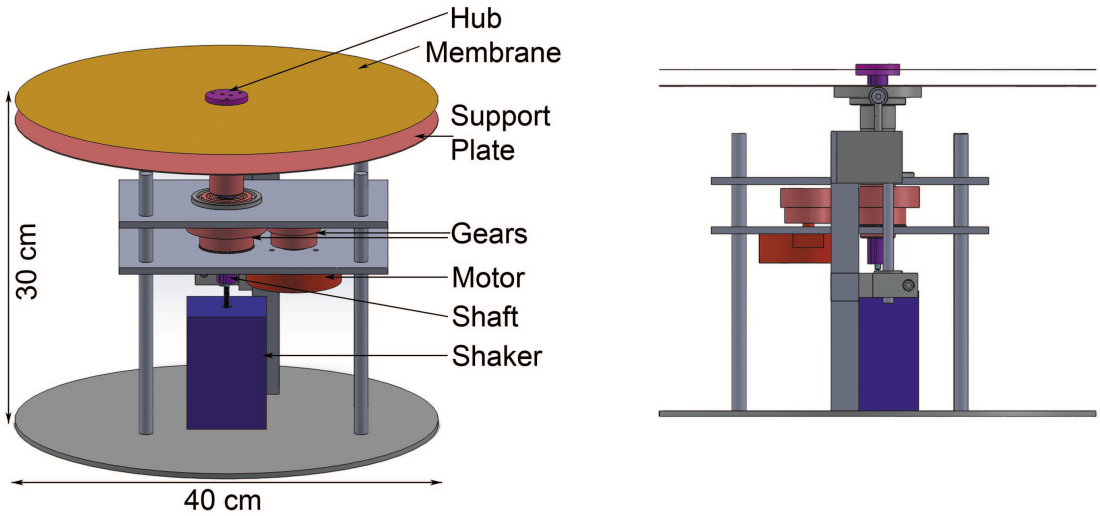

Figure 27: Views of experimental setup.

VII. Conclusion

Phased array antennas operating at 1 GHz have been considered and it has been shown that efficient performance requires that the antenna stays flat to an accuracy of a few centimeters. These antennas can be recalibrated electronically if they deform statically, but if the deformation occurs rapidly electronic correction becomes more challenging.

The case of spinning antenna structures has been considered and their dynamics have been investigated. For a diameter of 60 m it has been shown that a thin spinning structure can be modeled as a membrane when studying the linear dynamics. Notably, a criterion to scale from 60 m to a laboratory experiment scale has been determined, in terms of the stiffness parameter κ.

The dynamics of such a structure subject to a step perturbation at the hub have been investigated. We have found that the results of finite element simulations are sensitive to the integration scheme used and that it is difficult to recreate the full dynamics for the mesh and elements tested, as high frequencies are easily damped. This problem can be studied experimentally by spinning the structure fast enough that gravity effects become negligibly small. We have define the geometry and the experimental parameters to recreate experimentally the dynamics of such a structure. The design of an experimental setup that should be able to realize such an experiment, with appropriate flatness conditions, has been presented. The results of these experiments will be presented in future publications.

References

[1]L. Johnson, *Solar Sail Propulsion*. NASA Marshall Space Flight Center.

[2]C.A. Balanis, *Antenna Theory: Analysis and Design*.

[3]G. Oliveri, L. Poli and A. Massa, *Maximum efficiency beam synthesis of radiating planar arrays for wireless power transmission*. IEEE Transactions on Antennas and Propagation, Vol. 61, No. 5 (2013).

[4]W. Eversman, *Transverse vibrations of a clamped spinning membrane*. AIAA Journal, Vol. 6, No. 7 (1968), pp. 1395-1397.

[5]J.G. Simmonds, *The transverse vibration of a flat spinning membrane*. Journal of the Aerospace Sciences, Vol. 29, No. 1 (1962), pp. 16-18.

[6]A. Leissa, *Vibration of Plates*, NASA SP-160, 1969.

[7]A. Raman and C.D. Mote Jr, *Effects of imperfection on the non-linear oscillations of circular plates spinning near critical speed*, International Journal of Non-Linear Mechanics 36 (2001) 261-289.

[8]V. Ranjan and M.K. Ghosh, *Transverse vibration of spinning disk with attached distributed patch and discrete point masses using finite element analysis*, International Journal of Engineering, Science and Technology, Vol. 1, No. 1, 2009.

[9]C. Touzé, O. Thomas and A. Chaigne, *Asymmetric non-linear forced vibrations of free-edge circular plates. Part 1: Theory*, Journal of Sound and Vibration (2002) 258(4), 649-676

[10]C. Touzé, O. Thomas and A. Chaigne, *Asymmetric non-linear forced vibrationsof free-edge circular plates. Part 2: experiments*, Journal of Sound and Vibration (2002) 258(4), 649-676.

[11]M. Géradin and D. Rixen, *Mechanical Vibrations*, Wiley.

[12]Nobukatsu Okuizumi. *Forced vibration experiments of a rotating extremely thin circular membrane*, Mechanical Engineering Journal, Vol.1 1. No.5. 2014.